Earthq Eng & Eng Vib (2013) 12: 319-332 **DOI**: 10.1007/s11803-013-0174-0

Development of seismic fragility curves for low-rise masonry infilled reinforced concrete buildings by a coefficient-based method

Ray Kai Leung Su† and Chien-Liang Lee‡

Department of Civil Engineering, The University of Hong Kong, Hong Kong, China

Abstract: This study presents a seismic fragility analysis and ultimate spectral displacement assessment of regular low-rise masonry infilled (MI) reinforced concrete (RC) buildings using a coefficient-based method. The coefficient-based method does not require a complicated finite element analysis; instead, it is a simplified procedure for assessing the spectral acceleration and displacement of buildings subjected to earthquakes. A regression analysis was first performed to obtain the best-fitting equations for the inter-story drift ratio (IDR) and period shift factor of low-rise MI RC buildings in response to the peak ground acceleration of earthquakes using published results obtained from shaking table tests. Both spectral acceleration- and spectral displacement-based fragility curves under various damage states (in terms of IDR) were then constructed using the coefficient-based method. Finally, the spectral displacements of low-rise MI RC buildings at the ultimate (or near-collapse) state obtained from this paper and the literature were compared. The simulation results indicate that the fragility curves obtained from this study and other previous work correspond well. Furthermore, most of the spectral displacements of low-rise MI RC buildings at the ultimate state from the literature fall within the bounded spectral displacements predicted by the coefficient-based method.

Keywords: seismic; fragility analysis; masonry; spectral displacement

1 Introduction

Seismic vulnerability assessment is important for identifying the damage risk of a structure affected by ground motion of a given intensity. Analysis results can be used for damage and loss evaluations, disaster response planning, and retrofitting decision-making for civil structures. In this regard, fragility curves, which graphically represent the seismic risk of a structure, are promising for illustrating the probabilities of exceeding different prescribed damage states (or performance levels) as a function of the intensity measures (IMs) of an earthquake, such as the peak ground acceleration (PGA), spectral acceleration (S_a) or spectral displacement (S_d). The fragility analysis (Casciati and Faravelli, 1991) for evaluating the seismic damage risks of buildings (Mosalam *et al*., 1997; Cornell *et al*., 2002; Lang and Bachmann, 2004; Akkar *et al*., 2005; Kircil and Polat, 2006; Ramamoorthy *et al*., 2006; Ellingwood *et al*., 2007; Lagaros, 2008; El Howary and Mehanny, 2011; Seyedi *et al*., 2010), bridges (Shinozuka *et al*., 2000a; Shinozuka *et al*., 2000b; Karim and Yamazaki, 2001; Karim and Yamazaki, 2003; Choi *et al*., 2004; Nielson and DesRoches, 2007; Padgett and DesRoches, 2008; Pan *et al*., 2010), and laboratory equipment (Konstantinidis and Makris, 2009) has been widely studied.

In previous studies, various pairs of structural responses (e.g., the maximum inter-story drift ratio, IDR) and corresponding IMs are typically obtained by nonlinear time history analysis (NTHA), pushover analysis (POA) (ATC, 1996; Fajfar and Gašperšič 1996; Chopra and Goel, 1999; Fajfar, 2000; Chopra and Goel, 2002; Kalkan and Kunnath, 2007) or incremental dynamic analysis (IDA) (Vamvatsikos and Cornell, 2002; Han and Chopra, 2006). IDA is a parametric analysis method by which a representative structural model is subjected to a suite of selected ground motion records with multiple scaled intensity levels, thus producing demand (or capacity) prediction curves as a function of the IMs. In the fragility analysis, the demands of structures are often assumed to be lognormally distributed (Cornell *et al*., 2002) such that the relationship between the demand and IMs can be predicted by a power model or two-parameter model (Cornell *et al*., 2002; Karim and Yamazaki, 2003; Choi *et al*., 2004; Ramamoorthy *et al*., 2006; Ellingwood *et al*., 2007; Nielson and DesRoches, 2007; Padgett and DesRoches, 2008; Konstantinidis and Makris, 2009;

Correspondence to: Ray Kai Leung Su, Department of Civil Engineering, The University of Hong Kong, Hong Kong, China
Tel: +852-28592648; Fax: +852-25595337
E-mail: klsu@hkucc.hku.hk
†Associate Professor; ‡Postdoctoral Fellow

Supported by: the Research Grants Council of the Hong Kong SAR under Project No. HKU7166/08E and the Sichuan Earthquake Roundtable Fund of the University of Hong Kong
Received May 14, 2012; **Accepted** March 2, 2013

Pan *et al*., 2010). Based on the lognormal distribution assumption, the scatter plots of the demands of structures and corresponding IMs are typically represented on a logarithmic scale; thus, a regression analysis can be used to obtain the best-fitting linear regression equation, bilinear regression equation (Ramamoorthy *et al*., 2006), or quadratic regression equation (Pan *et al*., 2010) to represent the trend of these data (or the power model). The logarithmic median (varying with the IM) or mean value and a logarithmic standard variation of the data with respect to these regression equations can be obtained by a simple statistical analysis. The probability of exceeding different damage levels conditional on a specific IM can be determined once the logarithmic mean and standard deviation are found using the standard normal distribution function (Casciati and Faravelli, 1991). The damage states of structures are typically specified by various IDR levels corresponding to well-known qualitative performance levels, such as the immediate occupancy (IO) state, life safety (LS) state, and collapse prevention (CP) state, which are used for the performance-based design proposed and suggested by design guidelines (ATC, 1996; ASCE, 2000).

With the advancement of computational technologies, the demands (or capacities) of buildings and IMs can be determined through NTHA, POA, or IDA, which are likely to produce the best estimation of a structure's seismic response parameters. However, a detailed and time-consuming well-calibrated analytical finite element model of the building, together with the full-range nonlinear material properties of all structural components, should be constructed and obtained before conducting the nonlinear seismic assessment analysis. Recently, simplified coefficient-based procedures for assessing the seismic inter-story drift demand and capacity of structures have been studied extensively (Miranda, 1999; Lu *et al*., 2009; Gupta and Krawinkler, 2000; Zhu *et al*., 2007; Su *et al*., 2008; Tsang *et al*., 2009; Su *et al*., 2011; Lee and Su, 2012; Su *et al*., 2012). These coefficient-based methods typically focus on determining the seismic capacity or demand of structures in terms of the inter-story drift ratio or global roof drift ratio by multiplying several prescribed drift-related factors. The accuracy of these coefficient-based seismic assessment methods depends strongly on the proposed modification or on drift-related factors, which are often determined and calibrated through numerical simulation results obtained from the nonlinear time history analyses of buildings subjected to various earthquake motions. Furthermore, most finite element building models discussed in the literature are medium- or high-rise RC or steel frames without masonry or shear wall (SW) infills. Lee and Su (2012) calibrated a coefficient-based seismic assessment method that integrates drift-related factors and the spectral acceleration (or the seismic inherent strength) of structures using available shaking table test results with a special emphasis on low-rise MI RC buildings. However, their study did not investigate the spectral displacement of low-rise MI RC buildings subjected to earthquakes.

It has been widely accepted that spectral displacements or IDR can be closely correlated with seismic damage of structures. In this study, the coefficient-based method is adopted to obtain not only the spectral accelerations but also the spectral displacements of buildings subjected to earthquakes. This paper first relates the IDR and period shift factor (PSF, or the period lengthening factor due to structural damage) to the PGA through a regression analysis using the experimental results of low-rise MI RC buildings obtained from shaking table tests where applicable. The variability of the IDR and PSF of buildings subjected to earthquakes is taken into account by considering a shift of one standard deviation away from the best-fitting median regression curves (equations) instead of simply assigning a maximum bias value of 20% for both the IDR and PSF, as proposed by Lee and Su (2012). The construction of both spectral acceleration- and spectral displacement-based fragility curves under various damage states is then presented by using a suite of IDRs and spectral acceleration and displacement data that are numerically simulated by the coefficient-based method. Finally, the spectral displacements of low-rise MI RC buildings at the ultimate (or near collapse) state obtained from this paper and the literature are further compared to validate the accuracy and reliability of the simplified method for evaluating the seismic performance of buildings.

2 Simplified coefficient-based method

Assuming that the floor diaphragms have been provided with sufficient steel reinforcement to prevent premature tearing failure of the floors and sufficient steel reinforcement has been added to avoid tensile failure of tie columns (Su *et al*., 2011), the spectral displacement demand (S_d) of the first-mode dominant low-rise building at a certain loading state can be represented as Eq. (1) according to the building model illustrated in Fig. 1

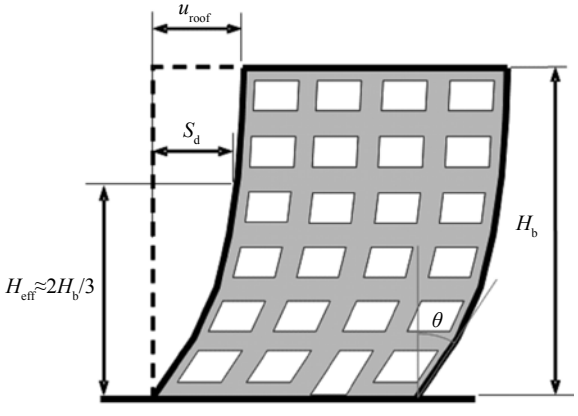

Fig. 1 Deformation model of a low-rise MI RC building

(Zhu *et al*., 2007; Su *et al*., 2008; Tsang *et al*., 2009; Su *et al*., 2011; Lee and Su, 2012; Su *et al*., 2012):

$$S_{\mathrm{d}} = \frac{H_{\mathrm{b}}\theta}{\lambda} \tag{1}$$

where λ is the drift factor; H_{b} is the height of the building; and θ is the maximum localized IDR corresponding to a certain loading state (or PGA). The spectral acceleration demand (S_{a}) can be related to S_{d} as follows:

$$S_{\mathrm{a}} = S_{\mathrm{d}}\left(\frac{2\pi}{T_{\mathrm{e}}}\right)^2 = \frac{H_{\mathrm{b}}}{T_0^2}\frac{(2\pi)^2}{\lambda}\frac{\theta}{\beta^2} \tag{2}$$

where T_0 is the initial fundamental vibration period of the intact (undamaged) structure that behaves linearly under ground motions with small intensities; and β is the period shift factor (PSF), which accounts for the effect of period lengthening (stiffness deterioration) of the equivalent (or secant) fundamental (first-mode) vibration period $T_{\mathrm{e}}=\beta T_0$ from strong ground shaking. This study adopts Eqs. (1) and (2) to estimate the spectral displacement and acceleration demands of low-rise MI RC structures for any IDR demand. Moreover, the spectral displacement and acceleration demands obtained from Eqs. (1) and (2) for a specific IDR (θ) may be regarded as the spectral displacement and acceleration capacities if the IDR reaches a certain limit state (performance level).

3 Review of the fragility analysis procedure

In fragility analyses, it is typically assumed that the demand (D) of a structure is lognormally distributed (Cornell *et al.*, 2002; Konstantinidis and Makris, 2009), meaning that the lognormally distributed variable D is related to a normally distributed variable X by $\ln(D)$. Therefore, the demand is normally predicted using a power model (or two-parameter model) as follows (Cornell *et al.*, 2002; Konstantinidis and Makris, 2009):

$$D = a(\mathrm{IM})^b \tag{3}$$

where a and b are unknown regression coefficients.

The unknown coefficients a and b can be easily obtained through a regression analysis of the demand data, which are obtained experimentally or numerically from an NTHA, a POA, an IDA, or the proposed coefficient-based method, in the following logarithmic form:

$$X = \ln(D) = \ln(a) + b\ln(\mathrm{IM}) \tag{4}$$

The mean and standard derivation of X can be, respectively, estimated as (Konstantinidis and Makris, 2009)

$$m_X(\mathrm{IM}) = \ln(a\mathrm{IM}^b) \tag{5a}$$

$$\sigma_X = \sigma_{\ln D} = \sqrt{\frac{1}{n-2}\sum_{i=1}^{n}\left[\ln\left(\frac{\delta_i}{a\mathrm{IM}_i^b}\right)\right]^2} \tag{5b}$$

where δ is a demand value.

For the lognormally distributed random variable D, the fragility function (P_{f}), which provides the probability that the demand D will exceed a certain threshold or capacity, C, conditional on a given IM, can be represented as

$$P_{\mathrm{f}} \equiv P(D > C \mid \mathrm{IM}) = 1 - \Phi\left(\frac{\ln C - m_X(\mathrm{IM})}{\sigma_X}\right) = 1 - \Phi\left(\frac{1}{\sigma_X}\ln\frac{C}{a\mathrm{IM}^b}\right) \tag{6a}$$

$$\Phi\left(\frac{\ln C - m_X(\mathrm{IM})}{\sigma_X}\right) = \int_{-\infty}^{u}\frac{1}{\sqrt{2\pi}\sigma_X}\exp\left(-\frac{u^2}{2}\right)\mathrm{d}u \tag{6b}$$

$$u = (\ln C - m_X(\mathrm{IM}))/\sigma_X \tag{6c}$$

where Φ is the cumulative distribution function of a standard normal variable and has a mean of 0 and standard variation of 1.

Using Eq. (6), once the two parameters, m_X (varying with IM) and σ_X, of variable X are obtained, the fragility curves can be constructed for various damage states or capacities. The demand and capacity considered in this study are the IDR (θ), and the IM used is either S_{a} or S_{d}.

4 Spectral acceleration-based fragility analysis

Before performing the fragility analysis, this study first relates the IDR (θ) and PSF (β) to the PGA through a regression analysis using experimental results for low-rise MI RC buildings obtained from shaking table tests or pseudodynamic tests (Dolce *et al*., 2005; Tomaževič and Klemenc, 1997; Lee and Woo, 2002; Kwan and Xia, 1996; Tsionis *et al*., 2001; Pinto and Taucer, 2006), as summarized by Lee and Su (2012) through a literature review. The number of stories, model scale, model height, input ground motion information, PGA and IDR of the building models are presented in Table 1. Note that the analyzed buildings are regular and uniform in elevation (with minor variation in the story height) and the masonry infilled walls are continuous along the building height without the weak or soft story. Among them, buildings 2 and 7 possess window or door openings. Moreover, the confined masonry (CM) building with reinforced RC tie columns (building 2) conducted by Tomaževič and Klemenc (1997) was able to withstand strong earthquakes with PGA of 0.8g (at the peak load state) and would not collapse when subjected to earthquakes with PGA more than 1.3g. The results indicate that the design strength of the CM building "specimen" seems to be stronger than the real traditional CM buildings. Therefore, the experimental results of

this CM building specimen were considered comparable with those of the MI RC buildings and also adopted in this study to obtain the relationship between the IDR and PGA. Scatter plots of the IDR and PSF as a function of the PGA for MI RC buildings are shown in Fig. 2(a) and Fig. 3(a), respectively, in which the best-fitting median linear regression equations (on a logarithmic scale) for the MI RC building data are obtained as follows (Lee and Su, 2012):

$$\ln(\theta) = 1.73557 \times \ln(\text{PGA}) - 4.05467 \qquad (7a)$$

$$\ln(\beta) = 0.351036 \times \ln(\text{PGA}) + 0.650516 \qquad (7b)$$

To take the variability of the IDR and PSF of MI RC buildings with different design details subjected to various characteristics of earthquakes into account, this study also considers standard deviation values of σ = 0.8643 and σ = 0.1933 for the IDR and PSF, respectively, that are directly determined from the regression analysis. Figures 2(a) and 3(a) show that most of the experimental data fall within the upper- and lower-bounded linear regression curves (equations) that consider one positive standard deviation value and one negative standard deviation value, respectively, with respect to the median linear regression curves. Using Eqs. (7a) and (7b) and the standard deviation values, the scatter plots of the IDR and PSF with the PGA within the upper- and lower-bounded linear regression curves shown in Fig. 2(a) and Fig. 3(a) can be numerically simulated and are summarized in Fig. 2(b) and Fig. 3(b), respectively. Taking the IDR as an example, the increment of PGA (on a logarithmic scale) between -2.5 and 0.55 (as shown in Fig. 2(a)) considered in this study is 0.03. As a result, 100 PGA values within the range of -2.5 and 0.55 were simulated. For each specific PGA value, the corresponding IDR can be obtained by using the equation, $\ln(\theta)=1.73557\times\ln(\text{PGA})-4.05467+\sigma$, in which the standard deviation value is assumed to vary randomly between -0.8643 and 0.8643. The PSF with the PGA can be simulated by using a similar procedure. Note that around 400 data points (four sets of randomly varied standard deviation values between -0.8643 and 0.8643 are used) of the IDR and PSF ($\geq$1.0) with the PGA were simulated in this study. Despite the fact that the experimental IDRs as shown in Table 1 were mainly obtained from the three- and four-story building models with various scales and building heights, the simulated IDR (Fig. 2(b)) and PSF (Fig. 3(b)) as a function of PGA obtained from the regressional Eqs. 7(a) and 7(b) will also be used later in this study to compute the spectral accelerations and displacements of low-rise MI RC buildings with $2 \leq N \leq 5$ stories using Eqs. (1) and (2). The rationality of the assumption may be examined through a comparison of the results of the spectral displacements of low-rise MI RC buildings ($2 \leq N \leq 5$) at the ultimate state (or near collapse state) obtained from this study and the literature, as will be presented later.

As shown in Eq. (2), the initial period (T_0) and the drift factor (λ) of the buildings should be introduced to calculate the spectral accelerations of buildings when using the coefficient-based method. This study adopts empirical period formula ($T_0=0.0294H_b^{0.804}$), which provides good approximations of the fundamental vibration periods for MI RC buildings as indicated by Lee and Su (2012). Moreover, the drift factor of λ=2.49 calibrated by Lee and Su (2012) using published experimental data of low-rise MI RC buildings obtained from shaking tests is adopted to predict the spectral accelerations and displacements of low-rise MI RC buildings with stories (with a story height of 3 m) for any given IDR.

Figure 4 illustrates simulated scatter plots of the IDR with S_a (on a logarithmic scale) for buildings with $2 \leq N \leq 5$ stories, and the best-fitting median linear regression equations for these data are presented. The spectral acceleration S_a can be obtained by substituting the drift factor λ=2.49, the building height and initial vibration period (e.g., H_b=12 m, $T_0=0.0294\times12^{0.804}=0.217$ s for the four-story MI RC buildings), and the simulated IDR

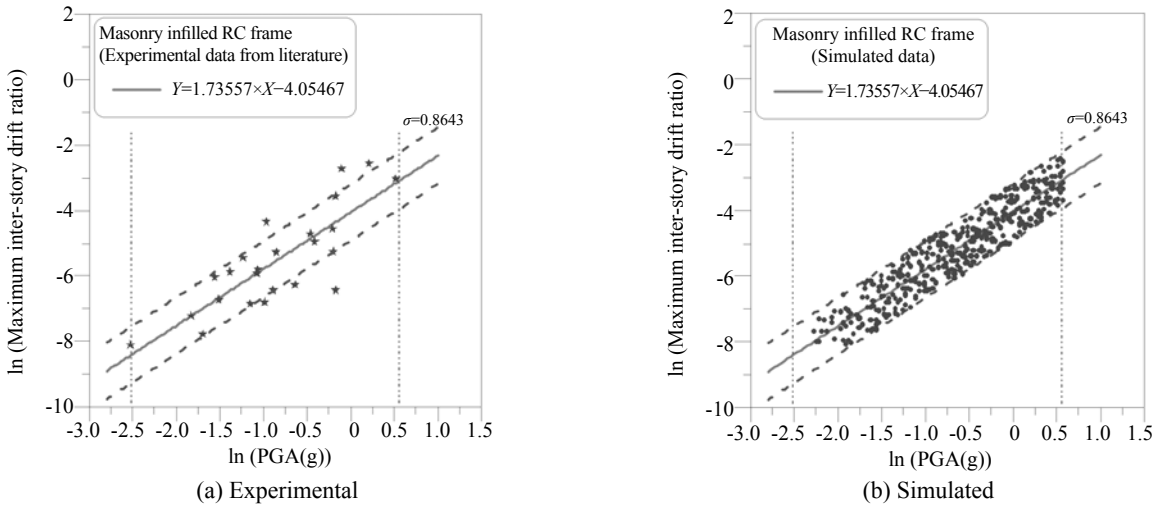

(a) Experimental (b) Simulated

Fig. 2 Variation of the maximum inter-story drift ratio with peak ground acceleration

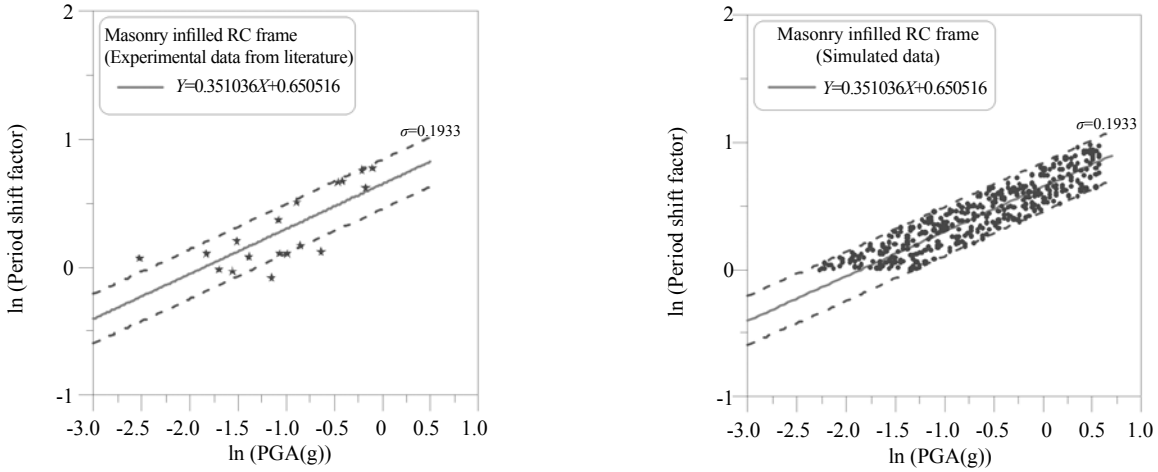

Fig. 3 Variation of the period shift factor with peak ground acceleration

Table 1 Summary of peak ground acceleration (PGA) and the corresponding θ of masonry infilled reinforced concrete buildings

Building models	Number of stories (N)	Model scale (1:S_l)	Model height (m)	PGA (g)	IDR θ
1. [Dolce *et al*., 2005] (Two-bay MI RC plane frame subjected to ground acceleration compatible with the EC8). Designed based on EC8.	3	1:3.3	3.225	0.08	0.0003
				0.16	0.0007
				0.22	0.0012
				0.34	0.0027
				0.63	0.0090
				0.90	0.0660
2. [Tomaževič and Klemenc, 1997] (Two identical three-dimensional confined masonry buildings subjected to 1979 Montenegro earthquake in longitudinal and transverse directions, respectively). Designed based on EC8.	3	1:5	1.584	0.84	0.0016
				1.67	0.0483
				0.82	0.0052
				1.23	0.0774
3. [Lee and Woo, 2002] (Two-bay fully masonry infilled plane RC frame subjected to 1952 Kern County earthquake-Taft N21E component). Designed based on Korean practice of non-seismic detailing.	3	1:5	2.220	0.18	0.00042
				0.32	0.00110
				0.37	0.00110
				0.53	0.00190
4. [Lee and Woo, 2002] (Two-bay partially masonry infilled RC plane frame subjected to 1952 Kern County earthquake-Taft N21E component). Designed based on Korean practice of non-seismic detailing.	3	1:5	2.220	0.21	0.0024
				0.25	0.0028
				0.34	0.0030
				0.43	0.0051
5. [Kwan and Xia, 1996] (Three-dimensional MI RC building subjected to 1940 El Centro earthquake in its short direction)	4	1:3	4.500	0.41	0.0016
				0.66	0.0071
				0.81	0.0105
6. [Tsionis *et al*., 2001] (Plane RC frame with two columns and two coupled shear walls subjected to artificial accelerogram conforming to the EC8). Designed based on EC8.	4	1:1	12.50	0.84	0.0286
7. [Pinto and Taucer, 2006] (Three-bay MI RC building subjected to European seismic hazard scenario). Designed based on EC8.	4	1:1	10.80	0.22	0.0012
				0.29	0.0043
				0.38	0.0129

(Fig. 2(b)) and PSF (Fig. 3(b)) data corresponding to each PGA for the low-rise MI RC buildings into Eq. (2). Based on the obtained median linear regression equations for the IDR with S_a, the median values (m_X(IM)) and the standard deviation (σ_X) can be obtained by using Eqs. (5a) and (5b), respectively. Taking the 4-story building (Fig.4) as an example, for S_a (i.e., IM)=1.0, the median value can be calculated as: m_X(IM)=Y=1.36049×1.0−5.14066=−3.78017, and the standard deviation is σ_X=0.3947. Note that the median value varies with S_a, while the standard deviation is a constant. With the obtained m_X(IM), σ_X, and the desired seismic performance level of buildings, C, the fragility values (P_f) corresponding to various S_a can be obtained by using Eqs. (6a)-(6c). From Eq. (6c), the u value can be determined for a given S_a, which in turn is substituted into Eq. (6b) to compute the cumulative distribution function (Φ). In this paper, the integral was numerically computed by a summation of the discretized value of $\exp(-u^2/2)/(\sqrt{2\pi}\sigma_X)$ between the interval [-100, u] with a constant increment of du=0.01. Further substituting the computed Φ value into Eq. (6a), the fragility value (P_f) for the given S_a can be obtained. Finally, the spectral acceleration-based fragility curve can be constructed by using the same procedure for each S_a value.

The spectral acceleration-based fragility curves for buildings with various numbers of stories under different performance levels are shown in Fig. 5, where the probability of exceedance tends to increase with the number of stories for a fixed spectral acceleration. The median spectral accelerations (with 50% fragility or 50% exceedance) of two-, three-, four- and five-story MI RC buildings are 1.36 g, 1.06 g, 0.89 g, and 0.78 g for the IO state (IDR=0.005); 2.25 g, 1.76 g, 1.48 g, and 1.29 g for the LS state (IDR=0.01); and 3.75 g, 2.93 g, 2.46 g, and 2.15 g for the CP state (IDR=0.02), respectively. The fragility curves for a four-story building obtained by the coefficient-based method and other published work (Goulet *et al*., 2007) are compared in Fig. 6, and it can be seen that the results correspond well when using the simplified coefficient-based method without a complicated finite element analysis. Note that the damage states of RC structures considered in this study are specified in FEMA-356 (ASCE, 2000): immediate occupancy (IO), where the structure has minimum damage and occupants have access to the structure following the earthquake event; life safety (LS), where the structure has significant damage, but the life safety of the occupants is preserved; and collapse prevention (CP), where the structure is on the verge of structural collapse. For RC structures, the qualitative

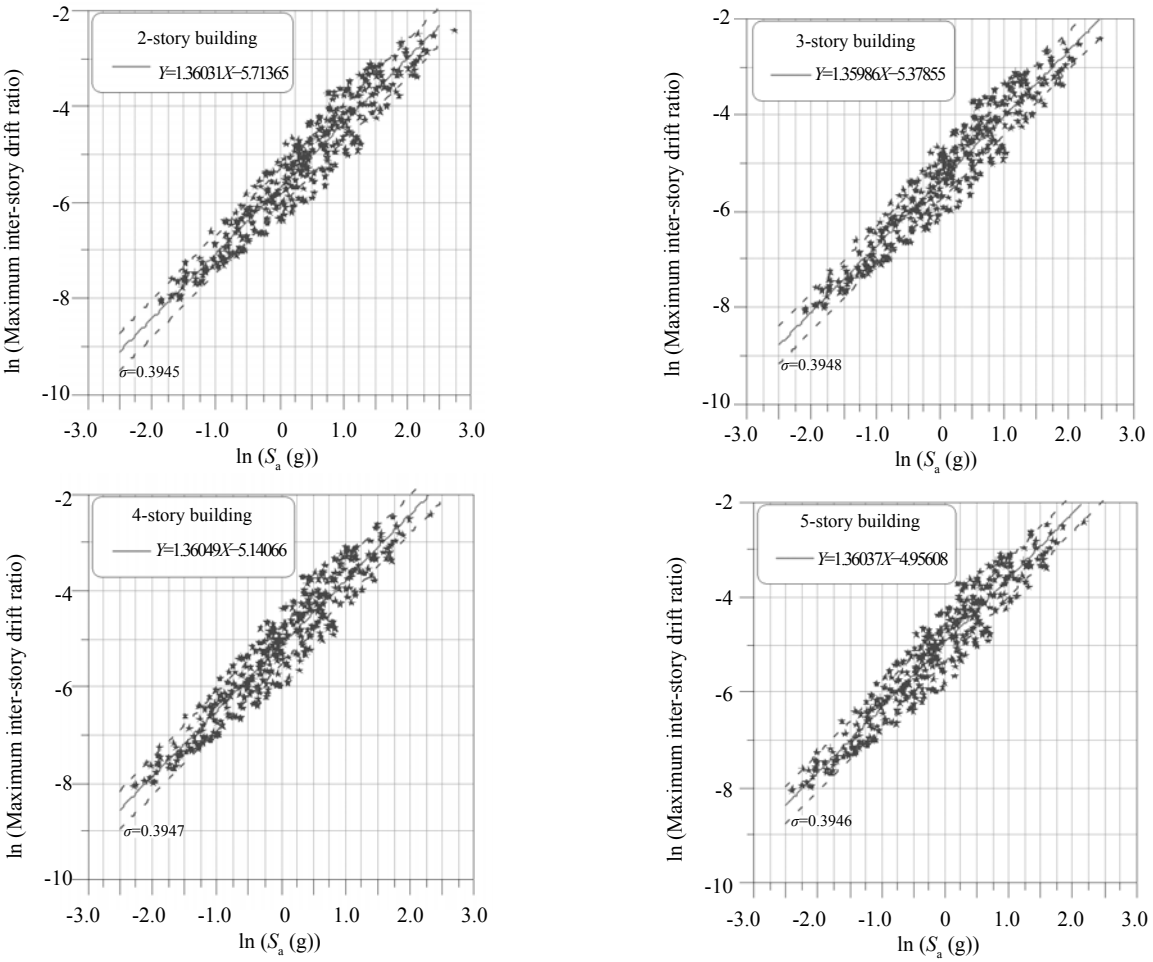

Fig. 4 Simulated scatter diagrams of the maximum inter-story drift ratio as a function of the spectral acceleration

damage states can be represented by the specific inter-story drift limits of 1%, 2%, and 4% for IO, LS, and CP, respectively (ASCE, 2000). These suggested limits are considered fairly representative for buildings that are properly designed for seismic loading. However, the IDR limits for LS and CP may not be conservative for old buildings and buildings with a gravity-load design due to insufficient column strength and section detailing. Thus, reduced drift limits of 0.5%, 1%, and 2%, which were suggested by Ramamoorthy *et al*. (2006), are also adopted in this study for the IO, LS, and CP performance levels, respectively.

As shown in Fig. 6(a), different variability or structural modeling uncertainties considered in the numerical model may lead buildings to have different collapse probabilities under a given damage state

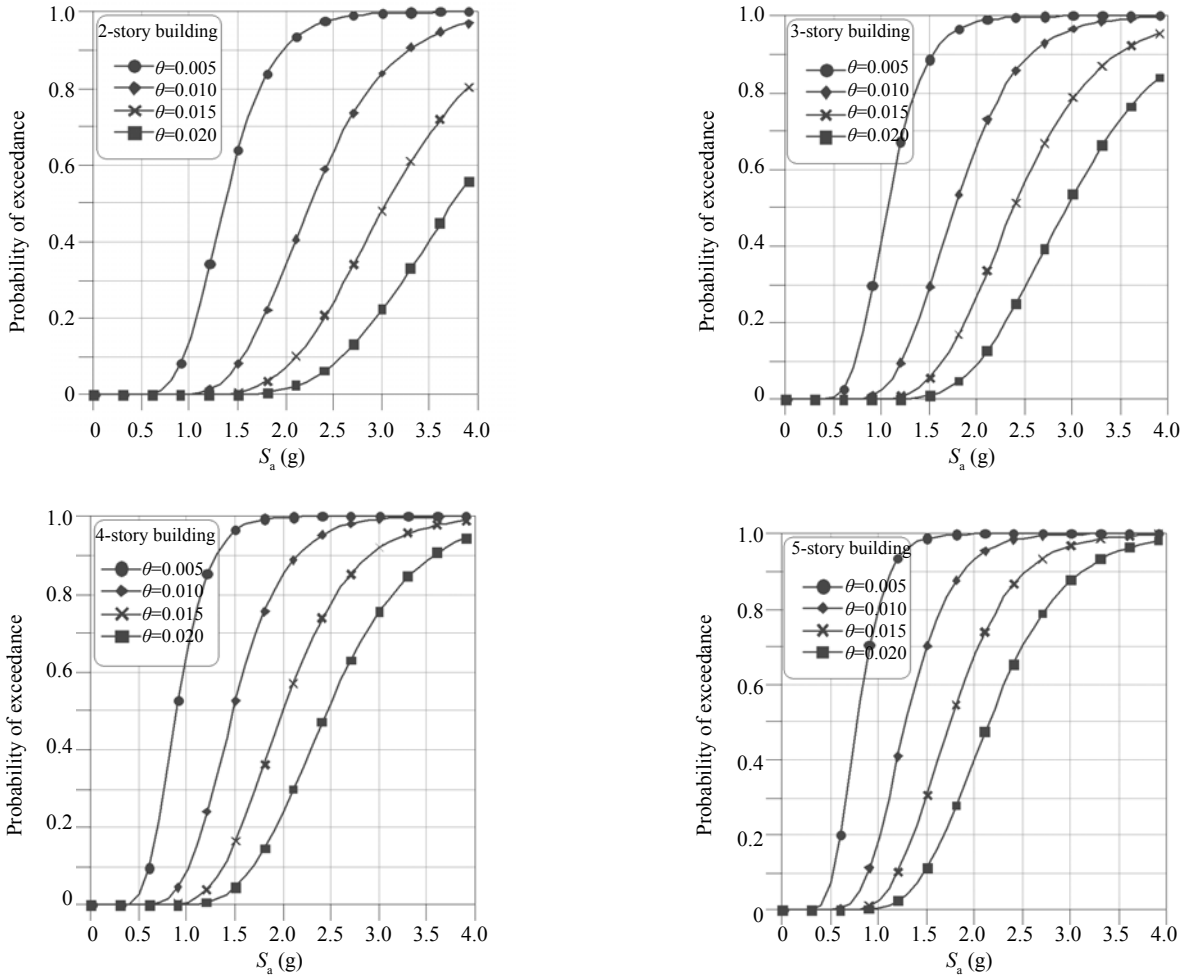

Fig. 5 Fragility curves of MI RC buildings in terms of the spectral acceleration

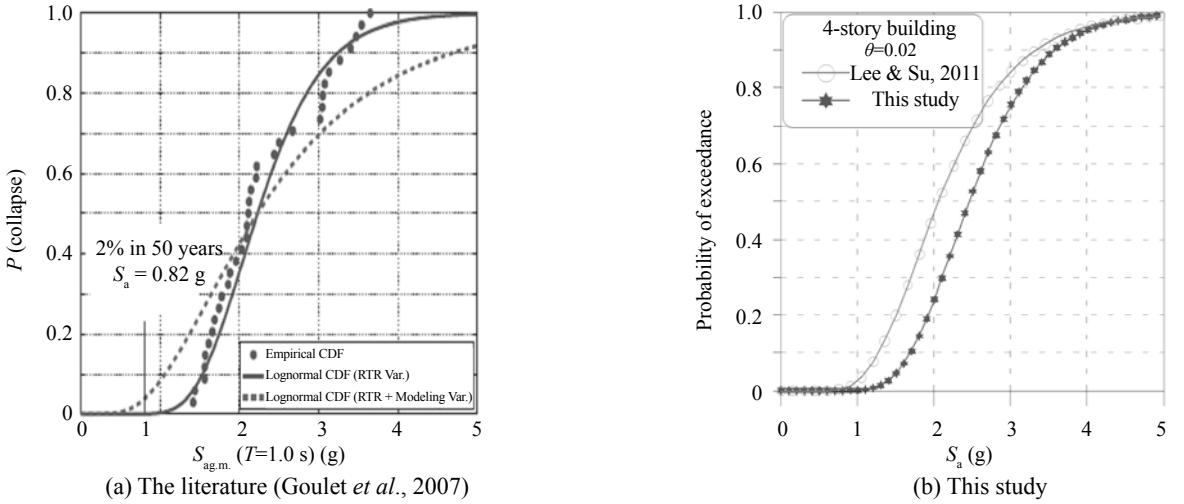

(a) The literature (Goulet *et al*., 2007) (b) This study

Fig. 6 Comparison of the fragility curves for a four-story building at the collapse state

(Goulet *et al*., 2007). This difference in collapse probabilities is due to the fact that the different levels of variability considered in the parameters of the numerical model may cause the median values to shift and the simulated results used to construct the fragility curves to disperse. Therefore, the fragility curve of four-story MI RC buildings at the CP state constructed by Lee and Su (2012) by assigning a maximum bias value of 20% for both the IDR and PSF of MI RC buildings subjected to earthquakes is also shown in Fig. 6(b) for comparison. The trend of the two fragility curves is fairly consistent, but the curve obtained by Lee and Su (2012) is higher than that obtained from the present study. As opposed to the aforementioned assumption made by Lee and Su (2012), this study considers the fact that the variations of the IDR and PSF used for obtaining the spectral accelerations (S_a) of low-rise MI RC buildings by the coefficient-based method fall within one standard deviation of the best-fitting median linear regression curves (Fig. 2(a) and Fig. 3(a)) as determined directly from the published experimental results. Furthermore, the best-fitting median linear regression curve for S_a and θ of the four-story MI RC buildings obtained in this study is $\ln(\theta)=1.36049\times\ln(S_a)-5.14066$, with a standard deviation of 0.39 (Fig. 4), while that obtained by Lee and Su (2012) is $\ln(\theta)=1.20494\times\ln(S_a)-4.78928$, with a standard deviation of 0.45 (1.15 times of that obtained from this study). From the two regression equations, it is observed that the IDR (θ) for a fixed S_a and the standard deviation shown in the previous work are both larger than those obtained in this study; this difference explains the reason why the fragility curve at the CP state obtained by Lee and Su (2012) is higher than that constructed from this study. Arbitrarily assigning a relatively large variability for the IDR and PSF of MI RC buildings used in the coefficient-based method may result in conservative fragility curves (collapse probabilities) of buildings; however, in many cases, it may not be possible to accurately determine the global variations of the parameters used in the numerical model beforehand. Thus, considering the maximum variability of the IDR and PSF within one standard deviation of the best-fitting median linear regression curves (IDR with PGA and PSF with PGA) determined directly using the published experimental results, as typically adopted in the statistical or engineering practice, is a more rational assumption and is adopted in this paper to obtain the satisfactory and reliable collapse probabilities (but not overestimated results) of buildings in the fragility analysis.

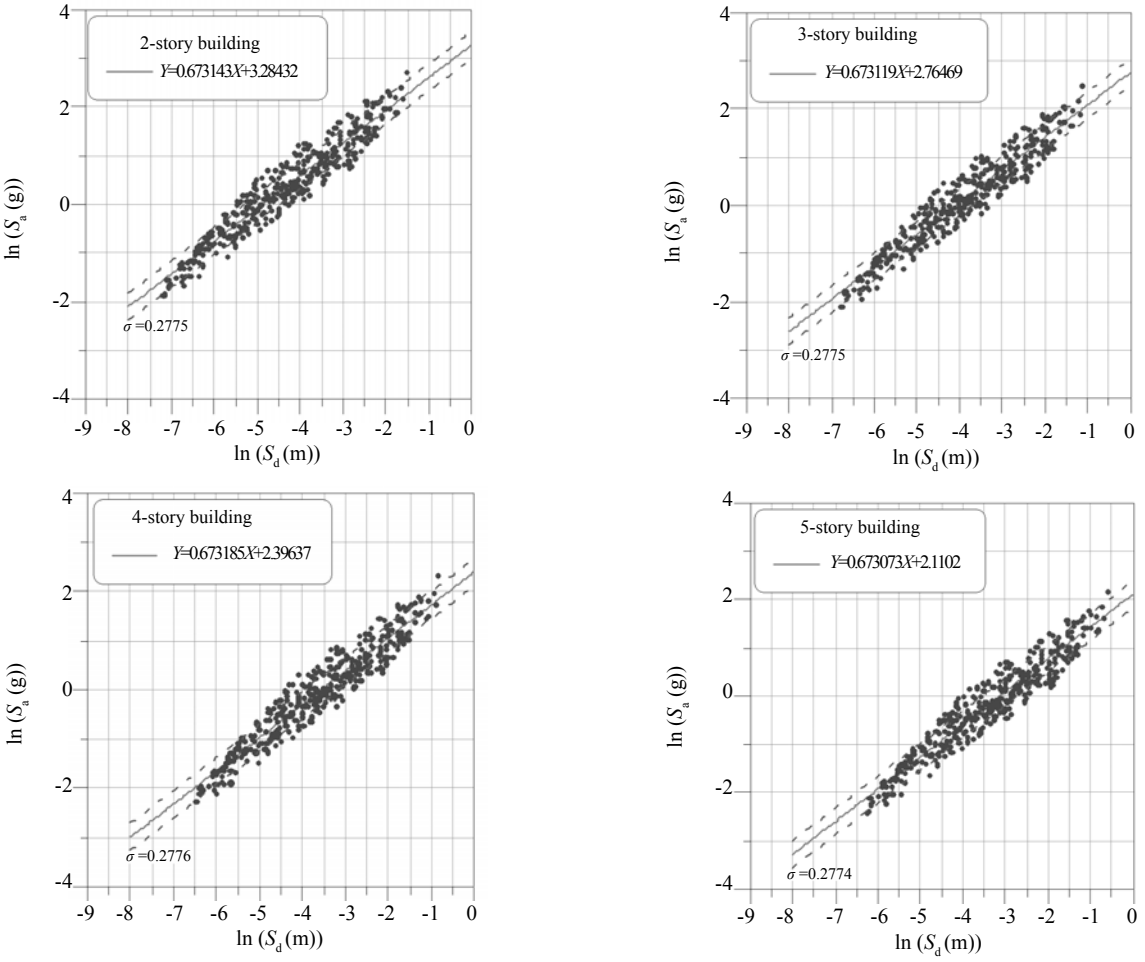

Fig.7 Simulated scatter diagrams of the spectral acceleration as a function of the spectral displacement

5 Spectral displacement-based fragility analysis

Spectral displacement-based fragility curves, as opposed to those that are based on spectral acceleration (or strength), are an alternative for evaluating the seismic performance of buildings. Thus, fragility curves in terms of spectral displacement for low-rise MI RC buildings are further constructed in this study. Figure 7 displays simulated scatter plots of S_a with S_d (on a logarithmic scale) for buildings with $2 \le N \le 5$ stories, from which the datum pair of S_d and S_a can be easily obtained, respectively, using Eqs. (1) and (2). From the relationship between the IDR and S_a as shown in Fig. 4, the ranges of the spectral acceleration corresponding to the various damage states of 0.5%, 1%, and 2% (IO, LS, and CP performance levels) in terms of the IDR are summarized in Fig. 8. Note that the variation range of spectral acceleration corresponding to a specific IDR is determined by a shift of one standard deviation from the median linear regression curve of the IDR with S_a. Taking the four-story building as an example, the median spectral accelerations corresponding to IDRs of 0.5%, 1%, and 2% are $e^{-0.1159}$=0.8906 g, $e^{0.3936}$=1.4823 g, and $e^{0.9031}$=2.4672 g, respectively. As a result, the fragility curves in terms of spectral displacement for low-rise MI RC buildings under different IDR levels can be constructed using the median linear regression equations for S_a and S_d (Fig.7) with the specific spectral acceleration levels corresponding to IDRs of 0.5%, 1%, and 2%, as illustrated in Fig. 9. The median spectral displacements (with 50% fragility or 50% exceedance) of 2-, 3-, 4- and 5-story MI RC buildings are 0.012 m, 0.018 m, 0.024 m, and 0.030 m for the IO state (IDR=0.005); 0.026 m, 0.038 m, 0.051 m, and 0.064 m for the LS state (IDR=0.01); and 0.054 m, 0.081 m, 0.108 m, and 0.136 m for the CP state (IDR=0.02), respectively.

6 Ultimate spectral displacement assessment

To further examine the reliability of the simplified coefficient-based method, the spectral displacements of low-rise MI RC buildings ($2 \le N \le 5$) at the ultimate state (or near collapse state) obtained from this study and the literature are compared. Note that the ultimate spectral displacements of low-rise MI RC buildings used in this study are those corresponding to IDR=0.02 (at the CP state), beyond which the MI RC buildings may fail. By simply substituting the spectral accelerations of low-rise MI RC buildings corresponding to the damage state with IDR=0.02 (Fig. 8), into the median linear regression equations of S_a with S_d (Fig. 7), the lower-

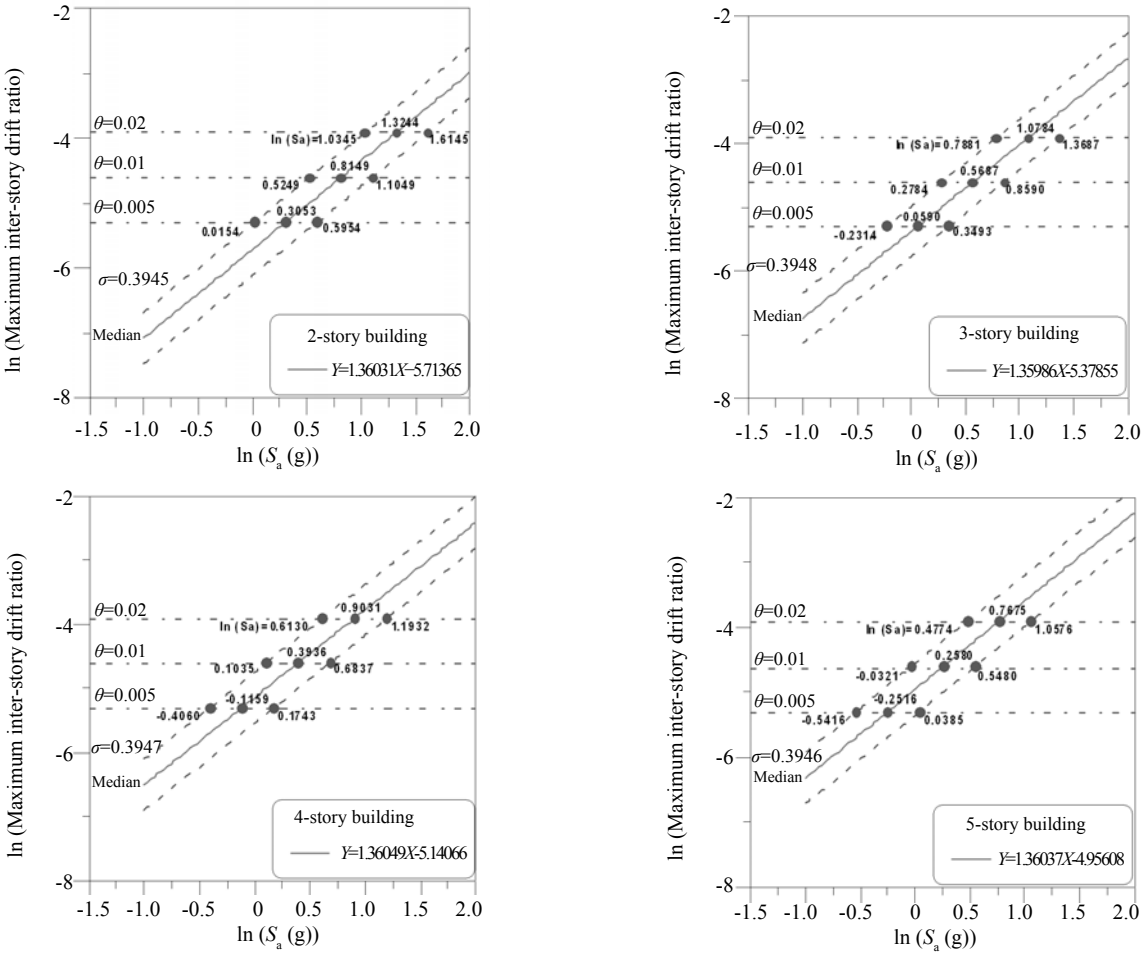

Fig. 8 Spectral accelerations corresponding to inter-story drift ratios of 0.005, 0.01, and 0.02

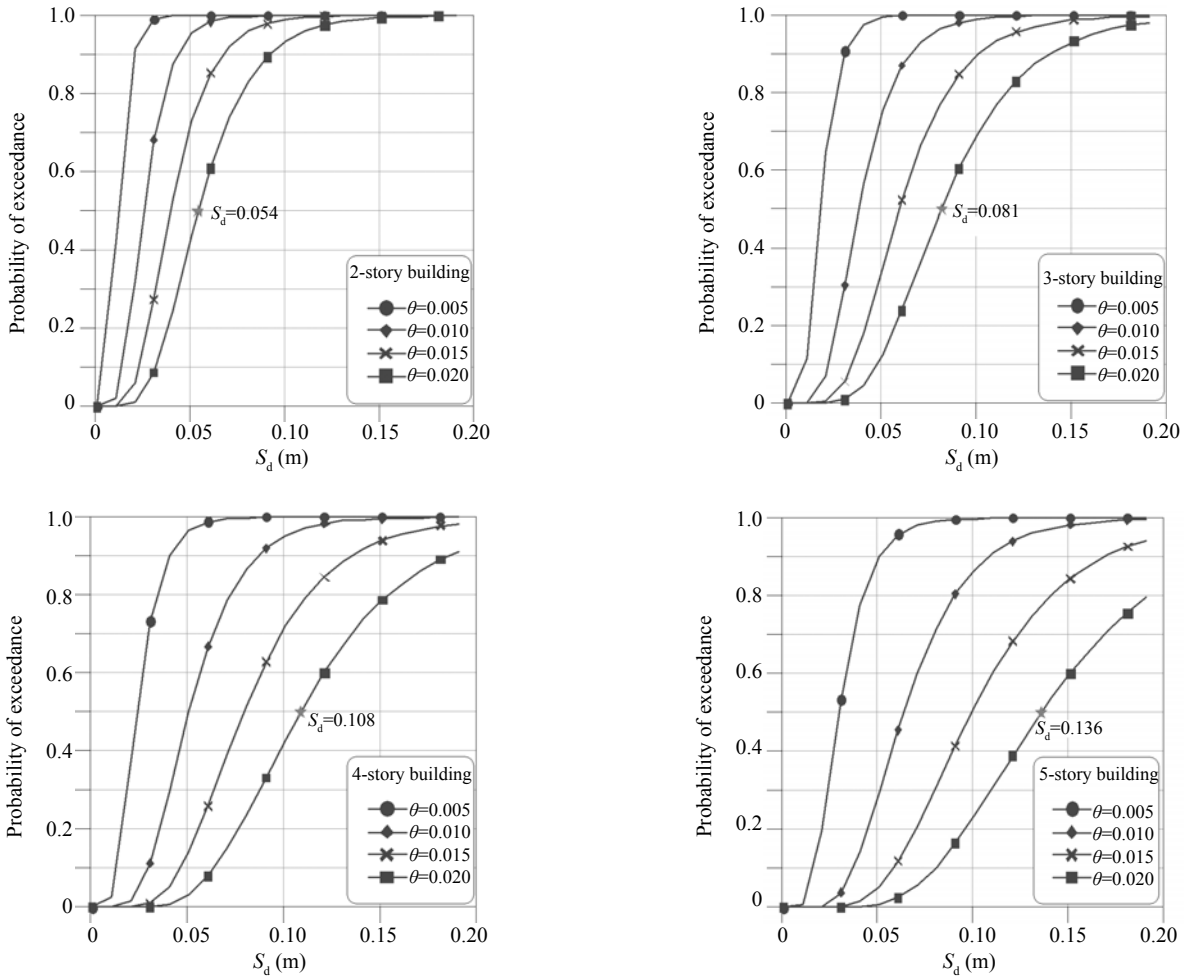

Fig. 9 Fragility curves for MI RC buildings in terms of the spectral displacement

bounded, median, and upper-bounded ultimate spectral displacements corresponding to IDR=0.02 can be obtained. Taking the four-story MI RC building as an example, by substituting the lower-bounded ($\ln(S_a)$=0.6130), median ($\ln(S_a)$=0.9031), and upper-bounded ($\ln(S_a)$=1.1932) spectral accelerations corresponding to IDR=0.02 (Fig. 8) into the linear regression equation of S_a with S_d on a logarithmic scale, $\ln(S_a)=0.673185\times\ln(S_d)+2.39637$ (Fig.7), for the four-story MI RC buildings, the lower-bounded, median, and upper-bounded ultimate spectral displacements at the CP state were predicted to be $\ln(S_d)$=-2.6492, -2.2182, and -1.7873 or = 0.0707 m, 0.1088 m, and 0.1674 m, respectively. Actually, the obtained median ultimate spectral displacements of the low-rise MI RC buildings were those corresponding to 50% fragility or 50% exceedance at the CP state (IDR=0.02) as obtained in Section 5 and highlighted by asterisks in Fig. 9. Figure 10 shows the upper-bounded, median, and lower-bounded spectral displacements of low-rise MI RC buildings with $2 \le N \le 5$ stories obtained at the CP state (IDR=0.02) using the coefficient-based method; the spectral displacements of low-rise MI RC buildings ($2 \le N \le 5$) at the ultimate (or near collapse) state obtained through a literature review (Porter, 2002; Kappos and

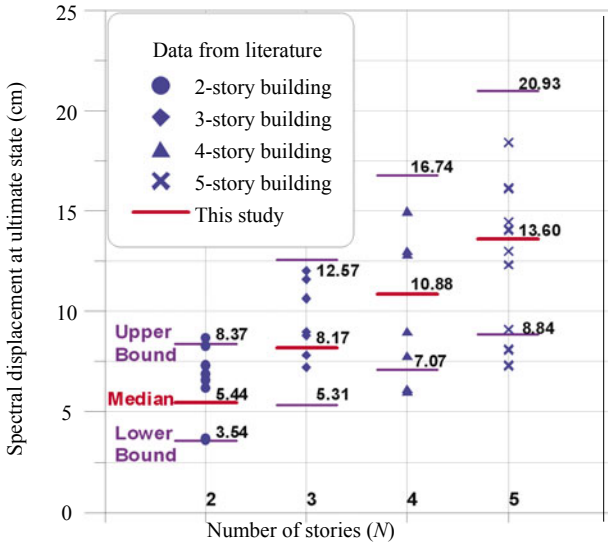

Fig. 10 Comparison of the spectral displacements at the ultimate state obtained from this study (IDR=0.02) and the literature

Panagiotopoulos, 2003; Das and Murty, 2004; Sung *et al*., 2006; Dolšek and Fajfar, 2008; Erberik, 2008; Yakut, 2008; Kaushik *et al*., 2009; Pham-Thi, 2009; Siahos and Dritsos, 2010; Bayhan and Gülkan, 2011; Marano *et al*.,

Table 2 Summary of the spectral displacements at the ultimate state obtained from the literature

	Literature	Number of stories (N)	Ultimate spectral displacement (cm) (S_d)
1	[Uva *et al*., 2012]	2	3.60
2	[Uva *et al*., 2012]	2	3.69
3	[Marano *et al*., 2011]	2	6.60
4	[Sung *et al*., 2006]	2	6.90
5	[Yakut, 2008]	2	7.30
6	[Porter, 2002]	2	8.30
7	[Kappos and Panagiotopoulos, 2003]	2	8.69
8	[Murty and Das, 2004]	3	7.20
9	[Murty and Das, 2004]	3	7.80
10	[Murty and Das, 2004]	3	8.80
11	[Erberik, 2008]	3	9.00
12	[Yakut, 2008]	3	10.65
13	[Porter, 2002]	3	11.60
14	[Murty and Das, 2004]	3	12.00
15	[Dolšek and Fajfar, 2008]	4	6.04
16	[Dolšek and Fajfar, 2008]	4	6.14
17	[Kaushik *et al*., 2009]	4	6.15
18	[Kappos and Panagiotopoulos, 2003]	4	7.77
19	[Siahos and Dritsos, 2010]	4	9.00
20	[Yakut, 2008]	4	12.84
21	[Porter, 2002]	4	15.00
22	[Bayhan and Gülkan, 2011]	5	7.30
23	[Bayhan and Gülkan, 2011]	5	8.10
24	[Bayhan and Gülkan, 2011]	5	9.10
25	[Marano *et al*., 2011]	5	12.98
26	[Erberik, 2008]	5	13.00
27	[Yakut, 2008]	5	14.06
28	[Pham-Thi, 2009]	5	14.46
29	[Pham-Thi, 2009]	5	16.08
30	[Porter, 2002]	5	18.40

2011; Uva *et al*., 2012), as summarized in Table 2, are also presented for comparison. Note that if the ultimate spectral displacements of buildings were not provided in the literature, the ultimate roof displacements (obtained from pushover analyses in the literature) divided by a modal participation factor of 1.3 for the first natural mode were used in this study. The comparison results demonstrate that most of the spectral displacements of low-rise MI RC buildings at the ultimate state obtained from the aforementioned work fall within the upper and lower bounds of spectral displacements predicted by the coefficient-based method using the CP state of IDR=0.02. This result indicates that in addition to constructing fragility curves, the simplified method can reliably yield the ultimate spectral displacements of low-rise MI RC buildings. Moreover, the comparison result may also reveal that the regressional Eqs. 7(a) and 7(b) obtained in this study using the published experimental results of shaking table tests can reasonably represent the IDR and PSF as a function of PGA for the low-rise MI RC buildings with $2 \le N \le 5$ stories as considered in this study.

7 Concluding remarks

This study presented a coefficient-based method for the seismic fragility analysis and ultimate spectral displacement assessment of low-rise MI RC buildings, which are subjected to higher earthquake forces than medium- and high-rise buildings in rock or soil conditions. The coefficient-based method does not require a finite element analysis and is a promising simplified, rapid manual procedure for estimating the spectral accelerations and displacements of buildings for a given inter-story drift ratio; in particular, the method can be used to quickly evaluate existing buildings and can be applied during the conceptual design phase of new buildings. This paper first related the inter-story drift ratio (θ) to the PGA and the period shift factor

(β) to the PGA through a regression analysis using the experimental results of MI RC buildings obtained directly from shaking table tests where applicable. The spectral acceleration- and spectral displacement-based fragility curves for various damage states constructed using a suite of inter-story drift ratios and spectral acceleration and displacement data that were simulated by the coefficient-based method are presented next. Finally, the spectral displacements of low-rise MI RC buildings at the ultimate state obtained from the coefficient-based method and a literature review were compared to validate the reliability of the simplified method. Based on the results of these analyses, the following conclusions may be drawn.

(1) Both the spectral accelerations and spectral displacements of low-rise MI RC buildings with $2 \leq N \leq 5$ stories at any loading state (or under a given inter-story drift ratio) can be obtained by the coefficient-based method if the parameters, such as the drift factor λ=2.49, period shift factor β (varying with PGA), and initial period T_0, are used.

(2) Fragility curves for low-rise MI RC buildings can be constructed by the proposed coefficient-based approach without the use of a complex finite element analysis. The comparison results indicate that the fragility curves obtained from this study and those from other previous studies for a four-story reinforced concrete building at the ultimate state correspond well. The obtained fragility curves can satisfactorily evaluate the vulnerability or the probability of exceedance for low-rise MI RC buildings under a given performance level in terms of the inter-story drift ratio.

(3) Most of the spectral displacements of low-rise MI RC buildings ($2 \leq N \leq 5$) at the ultimate (or near collapse) state from previous studies fall within the upper- and lower-bounded spectral displacements as predicted by the simplified coefficient-based method using the collapse prevention state of the inter-story drift ratio of 0.02; this result demonstrates that the simplified method can reliably yield the ultimate spectral displacement of low-rise MI RC buildings and may be a promising method for evaluating the seismic performance of buildings.

Acknowledgement

This research was supported by the Research Grants Council of the Hong Kong SAR (Project No. HKU7166/08E) and the Sichuan Earthquake Roundtable Fund of the University of Hong Kong.

References

Akkar S, Sucuoglu H and Yakut A (2005), "Displacement-based Fragility Functions for Low- and Mid-rise Ordinary Concrete Buildings," *Earthquake Spectra*, **21**(4): 901–927.

ASCE (2000), American Society of Civil Engineers, *Prestandard and Commentary for the Seismic Rehabilitation of Buildings* (*Report No. FEMA-356*), Washington, D.C.

ATC (1996), Applied Technology Council, *Seismic Evaluation and Retrofit of Concrete Buildings* (*ATC-40*), Redwood City, California.

Bayhan B and Gülkan P (2011), "Buildings Subjected to Recurring Earthquakes: A Tale of Three Cities," *Earthquake Spectra*, **27**(3): 635–659.

Casciati F and Faravelli L (1991), *Fragility Analysis of Complex Structural Systems*, Research Studies Press, England.

Choi E, DesRoches R and Nielson B (2004), "Seismic Fragility of Typical Bridges in Moderate Seismic Zones," *Engineering Structures*, **26**(2): 187–199.

Chopra AK and Goel RK (1999), "Capacity-demand-Diagram Methods for Estimating Seismic Deformation of Inelastic Structures: SDF System," *Report No. PEER-1999/02* (Pacific Earthquake Engineering Research Center), University of California, Berkeley.

Chopra AK and Goel RK (2002), "A Modal Pushover Analysis Procedure for Estimating Seismic Demands for Buildings," *Earthquake Engineering and Structural Dynamics*, **31**(3): 561–582.

Cornell CA, Jalayer F, Hamburger RO and Foutch DA (2002), "Probabilistic Basis for 2000 SAC Federal Emergency Management Agency steel moment frame guidelines," *Journal of Structural Engineering*, ASCE, **128**(4): 526–533.

Das D and Murty CVR (2004), "Brick Masonry Infills in Seismic Design of RC Frame Buildings: Part 2-Behaviour," *The Indian Concrete Journal*, **78**(8): 31–38.

Dolce M, Cardone D, Ponzo FC and Valente C (2005), "Shaking Table Tests on Reinforced Concrete Frames without and with Passive Control Systems," *Earthquake Engineering and Structural Dynamics*, **34**(14): 1687–1717.

Dolšek M and Fajfar P (2008), "The Effect of Masonry Infills on the Seismic Response of a Four-story Reinforced Concrete Frame-a Deterministic Assessment," *Engineering Structures*, **30**(7): 1991–2001.

El Howary HA and Mehanny SSF (2011), "Seismic Vulnerability Evaluation of RC Moment Frame Buildings in Moderate Seismic Zones," *Earthquake Engineering and Structural Dynamics*, **40**(2): 215–235.

Ellingwood RR, Celik OC and Kinali K (2007), "Fragility Assessment of Building Structural Systems in Mid-America," *Earthquake Engineering and Structural Dynamics*, **36**(13): 1935–1952.

Erberik MA (2008), "Fragility-based Assessment of Typical Mid-rise and Low-rise RC Buildings in Turkey," *Engineering Structures*, **30**(5): 1360–1374.

Fajfar P (2000) "A Nonlinear Analysis Method for Performance-based Seismic Design," *Earthquake Spectra*, **16**(3): 573–592.

Fajfar P and Gašperšič P (1996), "The N2 Method for the Seismic Damage Analysis for RC Buildings," *Earthquake Engineering and Structural Dynamics*, **25**(1): 31–46.

Goulet CA, Haselton CB, Mitrani-Reiser J, Beck JL, Deierlein GG, Porter KA and Stewart JP (2007), "Evaluation of the Seismic Performance of a Code-confirming Reinforced-concrete Frame Building-from Seismic Hazard to Collapse Safety and Economic Losses," *Earthquake Engineering and Structural Dynamics*, **36**(13): 1973–1997.

Gupta M and Krawinkler H (2000), "Estimation of Seismic Drift Demands for Frame Structures," *Earthquake Engineering and Structural Dynamics*, **29**(9): 1287–1305.

Han SW and Chopra AK (2006), "Approximate Incremental Dynamic Analysis Using Modal Pushover Analysis Procedure," *Earthquake Engineering and Structural Dynamics*, **35**(15): 1853–1873.

Kalkan E and Kunnath SK (2007), "Assessment of Current Nonlinear Static Procedures for Seismic Evaluation of Buildings," *Engineering Structures*, **29**(3): 305–316.

Kappos AJ and Panagiotopoulos CG (2003), "Inelastic Static Analysis of Infilled R/C Buildings," *Proceedings of the International Conference on Computational and Experimental Engineering and Sciences*, Corfu Island, Greece, Paper ID: 305.

Karim KR and Yamazaki F (2001), "Effect of Earthquake Ground Motions on Fragility Curves of Highway Bridge Piers Based on Numerical Simulation," *Earthquake Engineering and Structural Dynamics*, **30**(12): 1839–1856.

Karim KR and Yamazaki F (2003), "A Simplified Method of Constructing Fragility Curves for Highway Bridges," *Earthquake Engineering and Structural Dynamics*, **32**(10): 1603–1626.

Kaushik HB, Rai DC and Jain SK (2009) "Effectiveness of Some Strengthening Options for Masonry-infilled RC Frames with Open First Story," *Journal of Structural Engineering*, ASCE, **135**(8): 925–937.

Kircil MS and Polat Z (2006), "Fragility Analysis of Mid-rise R/C Frame Buildings," *Engineering Structures*, **28**(9): 1335–1345.

Konstantinidis D and Makris N (2009), "Experimental and Analytical Studies on the Response of Freestanding Laboratory Equipment to Earthquake Shaking," *Earthquake Engineering and Structural Dynamics*, **38**(6): 827–848.

Kwan KH and Xia JQ (1996), "Study on Seismic Behavior of Brick Masonry Infilled Reinforced Concrete Frame Structures," *Earthquake Engineering and Engineering Vibration*, **16**(1): 87–99. (In Chinese)

Lagaros ND (2008), "Probabilistic Fragility Analysis: A Tool for Assessing Design Rules of RC Buildings," *Earthquake Engineering and Engineering Vibration*, **7**(1): 45–56.

Lang K and Bachmann H (2004), "On the Seismic Vulnerability of Existing Buildings: A Case Study of the City of Basel," *Earthquake Spectra*, **20**(1): 43–66.

Lee CL and Su RKL (2012), "Fragility Analysis of Low-rise Masonry Infilled Reinforced Concrete Buildings by A Coefficient-based Spectral Acceleration Method," *Earthquake Engineering and Structural Dynamics*, **41**(4): 697–713.

Lee HS and Woo SW (2002), "Effect of Masonry Infills on Seismic Performance of A 3-story R/C Frame with Non-seismic Detailing," *Earthquake Engineering and Structural Dynamics*, **31**(2): 353–378.

Lu Y, Gu X and Wei J (2009), "Prediction of Seismic Drifts in Multi-story Frames with A New Story Capacity Factor," *Engineering Structures*, **31**(2): 345–357.

Marano GC, Greco R and Morrone E (2011), "Analytical Evaluation of Essential Facilities Fragility Curves by Using A Stochastic Approach," *Engineering Structures*, **33**(1): 191–201.

Miranda E (1999), "Approximate Seismic Lateral Deformation Demands in Multistory Buildings," *Journal of Structural Engineering*, ASCE, **125**(4): 417–425.

Mosalam KM, Ayala G, White RN and Roth C (1997), "Seismic Fragility of LRC Frames with and without Masonry Infill Walls," *Journal of Earthquake Engineering*, **1**(4): 693–720.

Nielson BG and DesRoches R (2007), "Analytical Seismic Fragility Curves for Typical Bridges in the Central and Southeastern United States," *Earthquake Spectra*, **23**(3): 615–633.

Padgett JE and DesRoches R (2008), "Methodology for the Development of Analytical Fragility Curves for Retrofitted Bridges," *Earthquake Engineering and Structural Dynamics*, **37**(8): 1157–1174.

Pan Y, Agrawal AK, Ghosn M and Alampalli S (2010), "Seismic Fragility of Multispan Simply Supported Steel Highway Bridges in New York State. II: Fragility Analysis, Fragility Curves, and Fragility Surfaces," *Journal of Bridge Engineering*, ASCE, **15**(5): 462-472.

Pham-Thi HC (2009), Seismic Performance Evaluation of RC Structures Designed by Vietnamese Code, *Master Thesis*, Department of Construction Engineering, National Taiwan University of Science and Technology, Taiwan.

Pinto A and Taucer F (2006), "Assessment and Retrofit of Full-scale Models of Existing RC Frames," in S. T. Wasti and G Ozcebe, editors, *Advances in Earthquake Engineering for Urban Risk Reduction*, Springer.

Porter KA (2002), "Seismic Vulnerability," in W. F. Chen and C Scawthron, editors, *Earthquake Engineering*

Handbook, Chapter 21, CRC Press.

Ramamoorthy SK, Gardoni P and Bracci JM (2006), "Probabilistic Demand Models and Fragility Curves for Reinforced Concrete Frames," *Journal of Structural Engineering*, ASCE, **132**(10): 1563–1572.

Seyedi DM, Gehl P, Douglas J, Davenne L, Mezher N and Ghavamian S (2010), "Development of Seismic Fragility Surfaces for Reinforced Concrete Buildings by Means of Nonlinear Time-history Analysis," *Earthquake Engineering and Structural Dynamics*, **39**(1): 91–108.

Shinozuka M, Feng MQ, Kim HK and Kim SH (2000a), "Nonlinear Static Procedure for Fragility Curve Development," *Journal of Engineering Mechanics*, ASCE, **126**(12), 1287–1295.

Shinozuka M, Feng MQ, Lee JH and Naganuma T (2000b), "Statistical Analysis of Fragility Curves," *Journal of Engineering Mechanics*, ASCE, **126**(12): 1224–1231.

Siahos G and Dritsos S (2010), "Procedural Assumption Comparison for Old Buildings via Pushover Analysis Including the ASCE 41 Update," *Earthquake Spectra*, **26**(1): 187–208.

Su RKL, Lam NTK and Tsang HH (2008), "Seismic Drift Demand and Capacity of Non-seismically Designed Buildings in Hong Kong," *Electronic Journal of Structural Engineering*, **8**: 110–120.

Su RKL, Lee YY, Lee CL and Ho JCM (2011), "Typical Collapse Modes of Confined Masonry Buildings under Strong Earthquake Loads," *The Open Construction and Building Technology Journal*, **5**(Supp1 1-M2): 50–60.

Su RKL, Lee CL and Wang YP (2012), "Seismic Spectral Acceleration Assessment of Masonry Infilled Reinforced Concrete Buildings by a Coefficient-based Method," *Structural Engineering and Mechanics*, **41**(4): 479–494.

Sung YC, Su CK, Wu CW and Tsai IC (2006), "Performance-based Damage Assessment of Low-rise Reinforced Concrete Buildings," *Journal of the Chinese Institute of Engineers*, **29**(1): 51–62.

Tomaževič M and Klemenc I (1997), "Verification of Seismic Resistance of Confined Masonry Buildings," *Earthquake Engineering and Structural Dynamics*, **26**(10): 1073–1088.

Tsang HH, Su RKL, Lam NTK and Lo SH (2009), "Rapid Assessment of Seismic Demands in Existing Buildings," *The Structural Design of Tall and Special Buildings*, **18**(4): 427–439.

Tsionis G, Negro P, Molina J and Colombo A (2001), "Pseodudynamic Tests on A 4-story RC Dual Frame Building," *Technical Report EUR19902EN* (European Laboratory for Structural Assessment, ELSA), Italy.

Uva G, Porco F and Fiore A (2012), "Appraisal of Masonry Infill Walls Effect in the Seismic Response of RC Framed Buildings: A Case Study," *Engineering Structures*, **34**: 514–526.

Vamvatsikos D and Cornell AC (2002), "Incremental Dynamic Analysis," *Earthquake Engineering and Structural Dynamics*, **31**(3): 491–514.

Yakut A (2008), "Capacity Related Properties of RC Frame Buildings in Turkey," *Journal of Earthquake Engineering*, **12**(S2): 265–272.

Zhu Y, Su RKL and Zhou FL (2007), "Cursory Seismic Drift Assessment for Buildings in Moderate Seismicity Regions," *Earthquake Engineering and Engineering Vibration*, **6**(1): 85–97.